

DARE2X

Decentralised Ammonia production from Renewable Energy utilising novel sorption-enhanced plasma-catalytic Power-to-X technology

D2.2 - Summary of experiments WP2 (methods, results, data)

Lead beneficiary: Danish Technological Institute
Author(s): Inês J. Andersen (DTI), Jens-Peter B. Haraldsted (DTI)

DATE: 30-09-2024

Abstract: Technical challenges prevent the realization of decentralized green NH_3 production. The DARE2X project aims to overcome these challenges by utilizing non-thermal plasma to drive the reaction with novel catalysts and sorption materials. The objectives of Work Package 2 are to optimize plasma catalysts using less critical raw materials, to further improve catalyst activity with the addition of promoters, to increase NH_3 yields by incorporating catalysts into sorption materials, and to upscale catalyst production. Catalyst materials were synthesized with a supercritical flow reactor and upscaled via wetness impregnation. Catalyst materials were benchmarked (Co, Ni, Cu, Ru, Pt, Fe, NiFe, NiCo, CoFe). The addition of promoters (Ca, Ba, La) and the incorporation of zeolite sorption materials were investigated.



This project has received funding from the European Union's Horizon Europe research and innovation programme under grant agreement No 101083905.



Part of this project has also received funding from UK Research and Innovation.

PROJECT DATA	
Project Acronym	DARE2X
Project Title	Decentralised Ammonia production from Renewable Energy utilising novel sorption-enhanced plasma-catalytic Power-to-X technology
Project number	101083905
Call identifier	HORIZON-CL5-2021-D3-03
Topic identifier	HORIZON-CL5-2021-D3-03-02 Next generation of renewable energy technologies
Type of action	Research and Innovation Actions
Project Duration	36 months (From 1 st October 2022)
Coordinator	Teknologisk Institut (DTI), Denmark - Christoffer Mølleskov Pedersen chm@teknologisk.dk
Website	www.dare2x.eu
DELIVERABLE DOCUMENT SHEET	
Deliverable No.	2.2
Deliverable title	Summary of experiments WP2 (methods, results, data)
Description	Summary of the experiments of WP2
WP No.	WP2
Related task	T2.1 - Synthesis and test of catalytic structures for plasma reactor. T2.3 - Improve catalyst performance with promoters. T2.4 - NH ₃ synthesis catalyst with incorporated sorption material. T2.5 - Upscale catalyst production for plasma-reactor
Lead Beneficiary	1) Danish Technological Institute
Author(s)	Inês J. Andersen (DTI), Jens-Peter B. Haraldsted (DTI), Matej Huš (NIC)
Contributor(s)	Matej Huš (NIC), Christoffer M. Pedersen (DTI)
Type ¹	R
Dissemination Level ²	Public
Language	English – GB

¹ R: Document, report; DEM: Demonstrator, pilot, prototype; DEC: Website, video etc., DATA: Data sets; DMP: Data management plan; ETHICS; SECURITY; Other: Software, technical diagram, algorithms, models etc.

² PU: Public, fully open; SEN: Sensitive.

Due date	30/09/2023	Submission date	30/09/2023
DOCUMENT HISTORY			
DATE	VERSION	AUTHOR	COMMENT
10/10/2023	V1	DTI, Inês J. Andersen, Jens-Peter B. Haraldsted	Initial Draft
26/09/2024	V2	Jens-Peter B. Haraldsted (DTI)	Updated with remaining results from WP2
30/09/2024	V3	Christoffer M Pedersen (DTI)	Update and QA before release

Acknowledgement



Funded by
the European Union

This project has received funding from the European Union’s Horizon Europe research and innovation programme under grant agreement No 101083905.



UK Research
and Innovation

Part of this project has also received funding from UK Research and Innovation.

Disclaimer

Views and opinions expressed are however those of the author(s) only and do not necessarily reflect those of the European Union. Neither the European Union nor the granting authority can be held responsible for them.

All intellectual property rights are owned by DARE2X consortium members and are protected by the applicable laws. Reproduction is not authorised without prior written agreement.

The commercial use of any information contained in this document may require a license from the owner of that information.

For citation purposes: *“Name of the authors, title of the report, DARE2X Project number 101083905, year of publication, page number, Name of the Beneficiary institution”.*



Funded by
the European Union

This project has received funding from the European Union’s Horizon Europe research and innovation programme under grant agreement No 101083905.



UK Research
and Innovation

Part of this project has also received funding from UK Research and Innovation.



ABBREVIATIONS AND ACRONYMS

EC	European Commission	CA	Consortium Agreement
GA	Grant Agreement	GDPR	General Data Protection Regulation



This project has received funding from the European Union's Horizon Europe research and innovation programme under grant agreement No 101083905.



Part of this project has also received funding from UK Research and Innovation.

TABLE OF CONTENTS

ABBREVIATIONS AND ACRONYMS	4
1. Introduction	6
2. Additional results from DFT screening study	8
3. Synthesis of Co-based catalysts	10
4. Synthesis of Ni-based catalysts	14
5. Synthesis of Cu-based catalysts	17
6. Synthesis of Pt-based catalysts	20
7. Synthesis of Ru-based catalysts	21
8. Plasma Activities of Co, Ni, Cu, Pt, Ru.....	22
9. Catalysts using sorption materials.	24
10. Synthesis of catalyst alloys with promoters.....	29
11. Synthesis of single atom and cluster catalysts.	32
12. Zeolites 5A and promoted 4A.....	34
13. Upscaled synthesis	37

1. Introduction

WP2 focuses on the development of efficient catalytic materials. The first task of WP2 (T2.1) focuses on the development of synthesis conditions for the preparation of immobilized particles of a metal of interest (Ni, Co, Cu, Pt and Ru) on a non-sorption material (alumina, carbon black and MgO). In this way the benchmarking of the most promising catalyst for the plasma catalytic reaction is the most accurate. The development of task 2.1 uses chemical characterization tools to determine the composition, structure and phase of the prepared catalyst. This information provides feedback to improve synthesis design, as seen in Figure 1.1. X-ray diffraction (XRD), and scanning electron microscopy with energy dispersive X-ray spectroscopy (SEM/EDX) were the techniques mainly used for this chemical characterization.

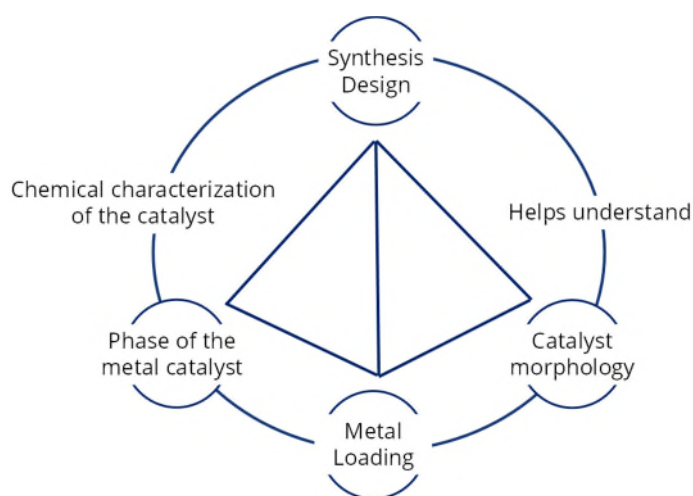


Figure 1.1. Schematic summarizing the strategy for the catalyst development from the WP2 tasks.

XRD is an X-ray based technique that is non-destructive. It allows the determination of the phase present in both solid and liquid samples, as well as the determination of crystal structure and orientation. XRD uses the constructive interference between X-rays and a sample. The wavelength of the X-rays used can be varied and is of the same order of magnitude of the distance between the atoms in a crystalline lattice, this interaction gives rise to a diffraction patterned that then can be analysed.

SEM/EDX is a technique used to obtain high-resolution images of surface topography. It works by using a focused electron beam to generate low energy secondary electrons, which are then measured to construct an image of the surface. The technique is highly sensitive to topographic features on the outermost surface and can achieve high spatial resolution due to the ability to focus the electron beam to a very small spot.

The synthesis we performed in a supercritical reactor. The supercritical reactors in DTI allow for the solvent pressurization and heating to their supercritical point making the synthesis of nanomaterials scalable and efficient. In Figure 1.2, there is a schematic of the reactor zones (Figure 1.2a) and reactor components (Figure 1.2b). The reactors are composed of 3 different

zones: zone of the precursor solution, zone of the support solution and the solvent zone. The precursor and support are pumped into the reactor by vacuum pumps. The two solutions meet in the mixing point, where a thermocouple is placed to determine the mixing temperature. The two solutions meet the preheated solvent at this point as well. The solvent is pumped into the same mixing point after being heated up. In the mixing point the cold support and precursor solutions meet the very hot solvent and are pumped into the reactor that is heated. The reactor column heating is called the vertical temperature. At the exit of the reactor there is a cooling system of water that allows the quick cooling of the product. The flow of precursor, support and solvent can be determined by weighing scales in ml/min.

The synthesis procedure allows the preparation of different combinations of metals and supports. Particle size can be controlled by tuning the pressure and temperature.

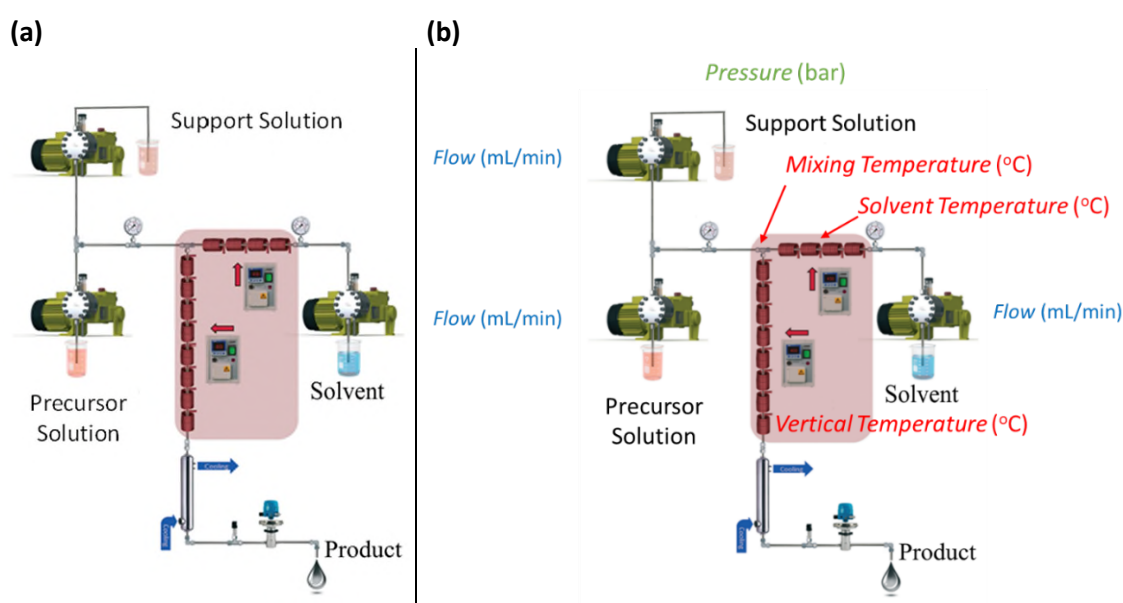


Figure 1.2. Schematic of the supercritical flow reactor where (a) summarizes the reactor zones, and (b) summarized the reactor components.

2. Additional results from DFT screening study

The computations were performed using plane-wave density functional theory (DFT) with the VASP 5.4.1 software package. Electron-ion interactions were modelled using the projector-augmented wave (PAW) method, while the RPBE functional was employed to account for electron exchange and correlation effects, with a plane-wave energy cut-off set to 500 eV. To account for dispersion forces, Grimme's D3 dispersion correction was applied along with dipole corrections. Initial transition states were located using the nudged elastic band (NEB) method and subsequently refined with the dimer method, applying a force convergence criterion of 0.05 eV/Å.

Vibrational frequency analysis for reaction rate calculations was carried out via the finite difference method, using the Hessian matrix and a displacement of 0.01 Å under the harmonic oscillator approximation, leveraging partition functions. Spin-polarized calculations were included for molecular oxygen adsorption and dissociation on all catalysts, as well as for all reaction steps on cobalt (Co) and nickel (Ni) surfaces.



Figure 2.1. Dissociative reaction mechanism for ammonia production.

The goal of computationally-driven catalyst design is a central focus in catalysis research, made increasingly attainable by advancements in computing power and theoretical methods. Key contributors to this progress include scaling relations, Brønsted–Evans–Polanyi (BEP) relations, and models like single-atom alloys (SAA), which have greatly enhanced computational catalyst design. While scaling and BEP relations provide a solid theoretical framework for simplifying the description of catalytic properties across various materials, their typical use is in modelling specific rate-determining steps on fixed catalyst surfaces.

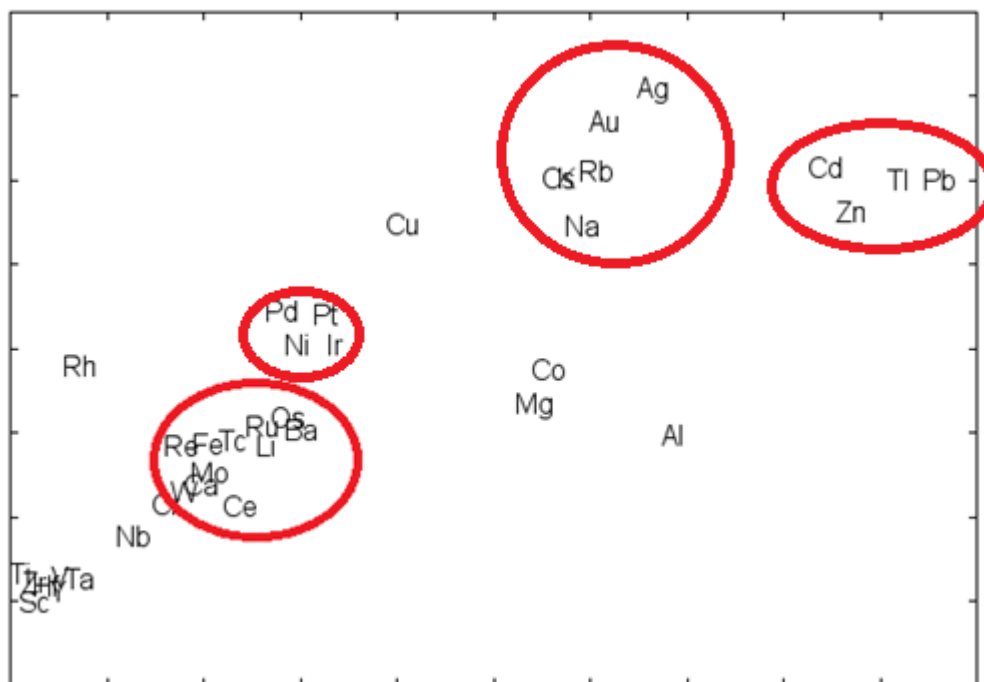


Figure 2.2. Different groups of metals, according to their affinity towards N_2 dissociation and H adsorption.

3. Synthesis of Co-based catalysts

The Co synthesis design was based on DTI's previous experience in logbooks from 2016. In the original synthesis, a Co alloy was prepared using CoCl and $(\text{Co}(\text{NO}_3)_2)$ as a precursor. When starting the first synthesis, the catalyst support used was a non-sorption material of $\theta\text{-Al}_2\text{O}_3$. The first steps were to determine the particle size of the support, where the support was initially clogging the reactor tubing. It was determined that the right particle size for the support was less than 1 μm . This size was achieved by milling the received alumina (Figure 3.1).

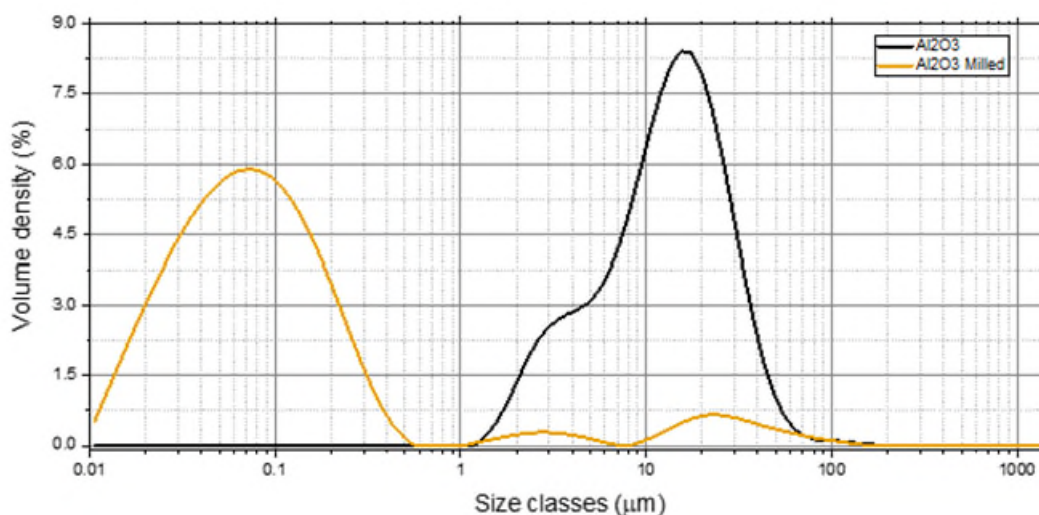


Figure 3.1. Size classes for Al_2O_3 powder 'as received' and milled.

The experimental design was started by investigating four different Co precursors:

1. Co nitrate ($\text{Co}(\text{NO}_3)_2$)
2. Co chloride (CoCl_2)
3. Co acetate ($\text{C}_4\text{H}_6\text{CoO}_4$)
4. Co acac ($\text{C}_{10}\text{H}_{14}\text{CoO}_4$)

D2X001 to D2X004 were discarded due to reactor clogging. It was also observed that the supernatant during the product centrifugation was of the same colour as the precursor indicating that there was no reaction taking place. Following the understanding of how to correctly prepare the support solution, the 4 precursors were tested a second time. D2X005 to D2X008 used ethanol as a solvent. These experiments did not result in a good product due to low mass yield. Furthermore, the precursor did not seem to precipitate, based on the colouring of the supernatant during upconcentration. The Co acac precursor was then discarded. Further testing was carried out using the 3 precursors with a lower vertical temperature (D2X010-D2X012) which resulted in the right aimed loading (10%) when using the nitrate and acetate precursors, but an unsuccessful loading when using chloride. This led to the exclusion of Co chloride as a precursor. Although D2X010 and D2X012 had the correct loading, the aimed phase was not realized. In these experiments, the phase was a Co oxide spinel structure (Co_2O_3), while the aimed result was a Co metallic phase.

Table 3.1. Summary of synthesis design for the Co catalysts.

Synthesis ID	Co Precursor	Support	Reducing Agent	Ratio (Reducing agent/Co precursor)	Water Solvent Content (%)	Tmix (°C)	Ts(°C)	Tv (°C)	P (bar)	Co (%)
D2X001	Nitrate	θ-Al ₂ O ₃			100		350	300	250	
D2X002	Chloride	θ-Al ₂ O ₃			100		350	300	250	
D2X003	Acetate	θ-Al ₂ O ₃			100		350	300	250	
D2X004	acac	θ-Al ₂ O ₃			100		350	300	250	
D2X005	Nitrate	θ-Al ₂ O ₃			100		350	300	250	
D2X006	Chloride	θ-Al ₂ O ₃			100		350	300	250	
D2X007	Acetate	θ-Al ₂ O ₃			100		350	300	250	
D2X008	acac	θ-Al ₂ O ₃			0		450	250	250	4.5
D2X009	Chloride	θ-Al ₂ O ₃			0		450	250	250	0.9
D2X010	Nitrate	θ-Al ₂ O ₃			100		350	250	250	12.2
D2X011	Chloride	θ-Al ₂ O ₃			100		350	250	250	0.8
D2X012	Acetate	θ-Al ₂ O ₃			100		350	250	250	12.9
D2X013	Nitrate	θ-Al ₂ O ₃			100		490	300	250	12.4
D2X014	Acetate	θ-Al ₂ O ₃			100		490	300	250	10.1
D2X015	Nitrate	θ-Al ₂ O ₃	Formic	1.25M	100		490	300	250	14.8
D2X016	Acetate	θ-Al ₂ O ₃	Formic	1.25M	100		490	300	250	7
D2X017	Acetate	θ-Al ₂ O ₃	Formic	1.25M	100		375	300	250	5.6
D2X018	Acetate	θ-Al ₂ O ₃	Glucose	0.2	0	253	490	253	250	
D2X019	Acetate	θ-Al ₂ O ₃	Glucose	0.05	0	274	490	274	300	
D2X020	Acetate	θ-Al ₂ O ₃	Formic	0.15	20	359	490	359	180	4
D2X021	Acetate	θ-Al ₂ O ₃			20	218	490	218	280	
D2X022	Acetate	θ-Al ₂ O ₃	Glucose	20	0	253	490	227	250	1.6
D2X023	Acetate	θ-Al ₂ O ₃	Glucose	5	0	274	490	245	300	2.8
D2X024	Acetate	θ-Al ₂ O ₃	Formic	15	0	394	490	292	150	3.6
D2X025	Acetate	θ-Al ₂ O ₃	Formic	1	20	359	490	391	180	6
D2X026	Acetate	θ-Al ₂ O ₃	Formic	10	30	339	490	251	200	4
D2X027	Acetate	θ-Al ₂ O ₃	Glucose	1	40	307	490	342	240	4.2
D2X028	Acetate	θ-Al ₂ O ₃		0	50	201	490	381	320	12
D2X029	Acetate	θ-Al ₂ O ₃	Glucose	5	60	369	490	364	240	5.6
D2X030	Acetate	θ-Al ₂ O ₃	Formic	5	60	281	490	434	300	8.5
D2X031	Nitrate	θ-Al ₂ O ₃	Glucose	10	70	314	490	248	280	0.9
D2X032	Nitrate	θ-Al ₂ O ₃	Formic	15	70	389	490	252	312	14.5
D2X033	Nitrate	θ-Al ₂ O ₃	Glucose	5	70	328	490	388	264	4.1
D2X034	Acetate	θ-Al ₂ O ₃	Formic	20	70	329	490	409	203	5.7
D2X035	Nitrate	θ-Al ₂ O ₃	Formic	1	70	363	490	435	253	15.2
D2X036	Acetate	θ-Al ₂ O ₃	Glucose	10	80	238	490	304	183	1.5

D2X037	Nitrate	θ-Al2O3		0	80	355	490	310	232	12
D2X038	Nitrate	θ-Al2O3		0	80	233	490	367	167	15.1
D2X039	Acetate	θ-Al2O3		0	80	377	490	429	290	10.4
D2X040	Nitrate	θ-Al2O3	Formic	1	90	279	490	422	185	9
D2X041	Nitrate	θ-Al2O3	Glucose	20	100	200	490	201	190	0.5
D2X042	Acetate	θ-Al2O3	Formic	10	100	298	490	271	215	2
D2X043	Nitrate	θ-Al2O3	Formic	20	100	251	490	277	214	4.8
D2X044	Acetate	θ-Al2O3	Glucose	15	100	259	490	324	270	1.7
D2X045	Nitrate	θ-Al2O3	Glucose	1	100	295	490	336	328	9
D2X046	Nitrate	θ-Al2O3		0	80	355	490	310	232	13.5
D2X047	Nitrate	θ-Al2O3	Formic	15	70	389	490	252	312	12.6
D2X048	Acetate	θ-Al2O3		0	50	201	490	381	320	11.3
D2X049	Acetate	θ-Al2O3	Formic	1	0	359	490	430	312	7
D2X050	Nitrate	θ-Al2O3		0	80	233	490	367	167	11.9
D2X051	Acetate	θ-Al2O3		0	80	377	490	429	290	12.4
D2X052	Nitrate	θ-Al2O3	Formic	1	70	363	490	435	253	13.6
D2X053	Nitrate	γ-Al2O3	Formic	15	70	389	490	252	312	10.6
D2X054	Nitrate	γ-Al2O4		0	80	355	490	310	232	9.8
D2X055	Acetate	γ-Al2O5		0	50	201	490	381	320	14.2
D2X056	Nitrate	Carbon Black	Formic	15	70	389	490	252	312	0.8
D2X057	Nitrate	Carbon Black		0	80	355	490	310	232	0.5
D2X058	Acetate	Carbon Black		0	50	201	490	381	320	0.7
D2X059	Nitrate	γ-Al2O3	Formic	20	70	350	490	350	200	11.3
D2X059V		γ-Al2O3					490			14.6
D2X060	Nitrate	γ-Al2O3	Formic	20	50	350	490	350	200	10.9
D2X060V		γ-Al2O3					490			13.9
D2X061	Nitrate	γ-Al2O3	Formic	20	30	350	490	350	200	12.5
D2X062	Nitrate	γ-Al2O3	Acetic	20	30	350	490	350	200	11.6
D2X063	Nitrate	γ-Al2O3	Acetic	20	70	350	490	350	200	13.8
D2X064	Acetate	Carbon Black			0	201	490	381	320	41.2
D2X065	Nitrate	γ-Al2O3	Glycerol	5	0	400	490	400	300	8.1
D2X066	Nitrate	γ-Al2O3	Glycerol	15	0	400	490	400	300	9.3
D2X067	Nitrate	Carbon Black	Glycerol	15	0	400	490	400	300	31.9
D2X068	Nitrate	γ-Al2O3	Glycerol	15	0	400	490	400	300	9.7
D2X069	Nitrate	γ-Al2O3			0	400	490	400	300	9.3
D2X070	Chloride	γ-Al2O3	Glycerol	15	0	250	490	200	250	0.5
D2X071	Chloride	γ-Al2O3	Glycerol	15	0	400	490	400	300	14.6

The next step was to achieve a metallic cobalt loading on alumina. For that, a new experiment set was prepared where the solvent temperature, and vertical heating was increased and the use of formic acid as a reducing agent was tested. The set of 4 experiments, resulted once again in the preparation of Co oxide. To better understand the limitations of the synthesis protocols, a design of experiments was set up (see D2X020-D2X045 in Table 3.2). This set of 25 experiments has a randomized variation of several parameters:

1. Nature of the precursor: Co nitrate ($\text{Co}(\text{NO}_3)_2$) and Co acetate ($\text{C}_4\text{H}_6\text{CoO}_4$)
2. Nature of the reducing agent: formic acid and glucose
3. Ratio of reducing agent/ precursor: 0,1, 5, 10, 15, 20.
4. Water solvent content.
5. Mixing temperature.
6. Vertical temperature.
7. Pressure.

In Figure 3.2, the oxidation state D2X020-071 was determined using XRD analysis. In orange is represented the full ethanol synthesis, and in green the full ethanol synthesis that use glycerol as a reducing agent. It was concluded from the design of experiments that the synthesis should be fully using ethanol, to generate as much hydrogen as possible to lower the oxidation number of the Co. It was also observed that formic acid and glucose were not advantageous as reducing agents. When investigating alternatives in the literature, glycerol seemed to be the ideal candidate for the transition metals synthesis.^{1,2} The use of glycerol and high temperature and pressure combined with previously discarded precursor of Co chloride resulted on metallic cobalt nanoparticles on alumina. In conclusion, the design of experiments resulted in knowledge of how to prepare, Co_2O_3 , CoAl_2O_4 , CoO , and Co (*metallic*) on various supports.

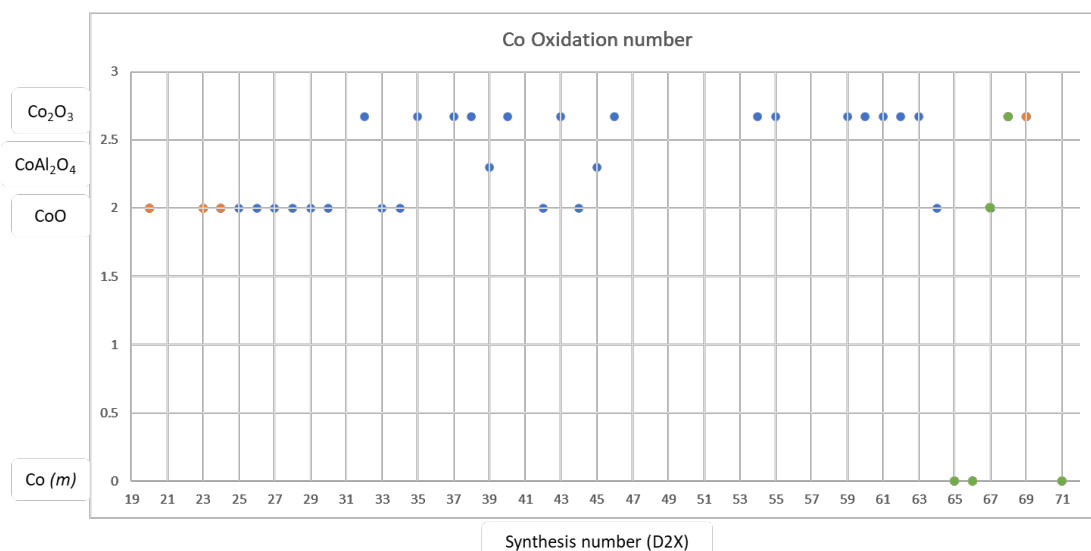


Figure 3.2. Oxidation number of cobalt species (O^{-3}) in the various synthesis (ranging from D2X19-71).

Figure 1

4. Synthesis of Ni-based catalysts

The nickel synthesis design was based on two different synthesis found in the DTI's logbooks (28-09-2016) and literature.² The logbook-based synthesis gave rise to D2X072 and D2X079, this synthesis used a NiCl₂ precursor and a lower T_{mix1} of 250 °C. D2X072 used a Ketjen Black support and D2X079 a γ-Al₂O₃ support. However, the two experiments gave rise to samples with very little nickel loading, and so there seemed little reason to investigate this synthesis strategy further.

The glycerol-based synthesis based on the literature seemed more promising, so it was explored extensively (D2X073-078, D2X080-089).² These glycerol-based synthesis experiments used:

1. higher T_{mix1} (aimed for 400 °C but achieved roughly 360 °C), unless stated otherwise.
2. Precursors and support flows of 10 ml/min, unless stated otherwise.
3. Glycerol, that degrades to yield hydrogen that subsequently reduces the Ni species into metallic nanoparticles. The glycerol was added with different molar ratios 0, 5, 15.
4. Two supports were used Ketjen Black and γ-Al₂O₃.
5. Finally, the aimed loadings were varied between 10 %wt., 30 %wt.

The D2X073-078 experiments using Ketjen Black consistently resulted in lower Nickel loadings of roughly 2/3 of the aimed Loading. In contrast, the D2X080-085 experiments using γ-Al₂O₃ consistently reached their aimed loadings. The D2X083 and D2X085 had exceeded their aimed loadings, but this is generally understood to be an issue with the precursor pumps delivering a consistent flow on that day (05-04-2023). Particularly with D2X083 that had a very low mass yield but a nickel loading of 47 %wt., suggesting the precursor pump delivering the γ-Al₂O₃ dispersion had slowed down. Nevertheless, the D2X073-078 and D2X080-085 experiments suggest that the Ketjen Black support interferes with the reduction of Ni species to Ni nanoparticles dispersed on a support. It is speculated that the reducible functional groups on the carbon (alcohols, amines, etc.) compete with Ni species to react with the available hydrogen but this is possibly refuted by the fact that varying molar ratios of glycerol do not seem to have a significant effect on the loading efficiency. The XRD analysis showed that D2X073-078 and D2X080-085 experiments yielded Ni particles of around 20-35 nm (diameter).

The D2X086-087 experiments tested higher precursor flows on a Ketjen Black support. The understanding from the Recycalyse project is that higher flows of pump 1+2 will significantly reduce the retention time in the reactor, and therefore yield more homogenous catalyst nanoparticle sizes. A lower T_{mix1} temperature of 300 °C is also explored. 17 ml/min flows were achieved while still maintaining a T_{mix1} of 300 °C. The resulting catalysts were still under the aimed loading, but D2X087 seemed a bit better, possibly attributed to the 5 molar equivalents of glycerol.

At this point, 15 molar equivalents of glycerol was exclusively used in the experiments with the assumption that it probably couldn't hurt the results, and there is a small chance that it might

be helpful. The D2X088-089 experiments were a repeat of D2X074 and D2X081 but with a lower T_{mix1} of 300 °C. This is to potentially deconvolute the D2X086-087 experiments where both higher flows and lower T_{mix1} were tested at once. The EDX results of D2X088-089 reinforce the same findings from the D2X073-078 and D2X080-085 experiments: the sample supported on γ - Al_2O_3 (D2X089) reached its aimed loading while the sample supported Ketjen Black (D2X088) resulted in lower Nickel loadings of roughly 2/3 of the aimed loading.

The serendipitous success of D2X071 (CoCl_2 on γ - Al_2O_3) led to the replicating this experiment with Ni (D2X090-091). The NiCl_2 precursor was therefore revisited with D2X090 on γ - Al_2O_3 support and D2X091 on KB support. The sample supported Ketjen Black (D2X091) follows the similar trend by resulting in lower Nickel loadings. Finally, the D2X074 experiment is replicated on MgO support in D2X092 and D2X093 with Ni loadings of 10 %wt. and 30 %wt., respectively. Similar to the experiments supported on Ketjen Black, the nickel loadings also did not reach their aimed loading (6.7 %wt. and 19.2 %wt.)

It has been concluded that glycerol is generally beneficial for the deposition of Ni at lower temperatures (D2X086-088) especially with the significant absence of Nickel loading in the D2X072+079 experiments. In contrast, glycerol seems inconsequential in experiments running at higher temperatures (D2X080-082 and D2X073-078). This is likely due to ethanol degrading to H_2 in significant amounts at higher temperatures, and glycerol ultimately becoming a redundancy. This contrast from the literature is understandable because they used glycerol in experiments with water as a solvent.²

In ambient conditions, glycerol can act as a weak reducing agent to form glycerone ($\Delta G = -10$ kJ/mol). Similarly, ethanol forms ethanal ($\Delta G = -35$ kJ/mol). At higher temperatures of 500 °C, the dry reforming of both glycerol and ethanol will begin yield H_2 in roughly ~ 0.75 and ~ 0.25 molar equivalents, respectively. For both aqueous glycerol and pure alcohols, it is thought that supercritical conditions of 350-400 °C is required to yield significant amounts of hydrogen to form nanoparticles in the metallic phase (Cu, Ni, Co). The supercritical point of ethanol is roughly 250 °C and 70 bar. This means in the lower temperature experiments, both glycerol and ethanol could potentially be acting as a traditional reducing agent similar to ambient conditions instead of a hydrogen source at >350 °C. Another possibility is the reforming of glycerol catalyzed by the inconel reactor, since it has been reported that Ni-Mg-Al will catalyze glycerol reforming to yield 1.7 molar equivalents at just 400 °C. Extrapolating this exponential trend down to 250-300 °C would yield roughly 0.50-1.00 molar equivalents of hydrogen. This could possibly explain the efficacy of glycerol in the experiments with lower temperatures, and also the improved loading efficiency in experiments using the γ - Al_2O_3 supports. This ultimately suggests ethanol and glycerol act mainly as a hydrogen source rather than a traditional reducing agent at the lower temperatures (250-300 °C) of supercritical ethanol, where the glycerol can yield significantly more amounts of hydrogen compared to ethanol.

Another theory was that the reducible functional groups on Ketjen Black compete with the metal for the reducing agents available. It is reported that Ketjen Black 300 has roughly 3% of alcohols and amines, which is roughly the molar equivalent of the missing Nickel loading in the Ketjen Black experiments. However, this theory seems less likely after the copper experiments.

Table 4.1. Summary of synthesis design for the Ni catalysts.

	Ni Precursor	Aimed Loading	Support	Reducing Agent	Ratio (Reducing agent/Ni precursor)	Solvent	Tmix	Tv	P	Loading (%)	Crystallite size (nm)
D2X072	NiCl ₂	20	Carbon Black			EtOH	250	250	250	0,0	Not enough metal
D2X073	Ni(NO ₃)	10	Carbon Black	glycerol	5	EtOH	400	400	300	6,6	19
D2X074	Ni(NO ₃)	10	Carbon Black	glycerol	15	EtOH	400	400	300	6,0	21
D2X075	Ni(NO ₃)	10	Carbon Black			EtOH	400	400	300	5,2	25
D2X076	Ni(NO ₃)	30	Carbon Black	glycerol	5	EtOH	400	400	300	20,4	28
D2X077	Ni(NO ₃)	30	Carbon Black	glycerol	15	EtOH	400	400	300	20,0	34
D2X078	Ni(NO ₃)	30	Carbon Black			EtOH	400	400	300	19,7	25
D2X079	NiCl ₂	20	γ-Al ₂ O ₃			EtOH	250	250	250	1,1	Not enough metal
D2X080	Ni(NO ₃)	10	γ-Al ₂ O ₃	glycerol	5	EtOH	400	400	300	9,6	20
D2X081	Ni(NO ₃)	10	γ-Al ₂ O ₃	glycerol	15	EtOH	400	400	300	10,6	23
D2X082	Ni(NO ₃)	10	γ-Al ₂ O ₃			EtOH	400	400	300	10,4	25
D2X083	Ni(NO ₃)	30	γ-Al ₂ O ₃			EtOH	400	400	300	47,0	23
D2X084	Ni(NO ₃)	30	γ-Al ₂ O ₃	glycerol	5	EtOH	400	400	300	31,9	30
D2X085	Ni(NO ₃)	30	γ-Al ₂ O ₃	glycerol	15	EtOH	400	400	300	37,9	25
D2X086	Ni(NO ₃)	20	Carbon Black			EtOH	300	300	300	11,8	23
D2X087	Ni(NO ₃)	20	Carbon Black	glycerol	5	EtOH	300	300	300	15,2	
D2X088	Ni(NO ₃)	10	Carbon Black	glycerol	15	EtOH	300	300	300	6,9	
D2X089	Ni(NO ₃)	10	γ-Al ₂ O ₃	glycerol	15	EtOH	300	300	300	9,9	
D2X090	NiCl ₂	10	γ-Al ₂ O ₃	glycerol	15	EtOH	400	400	300	15,9	26
D2X091	NiCl ₂	10	Carbon Black	glycerol	15	EtOH	400	400	300	4,3	Rough 15
D2X092	Ni(NO ₃)	10	MgO	glycerol	15	EtOH	400	400	300	6,7	Not enough metal
D2X093	Ni(NO ₃)	30	MgO	glycerol	15	EtOH	400	400	300	19,2	Rough 18

5. Synthesis of Cu-based catalysts

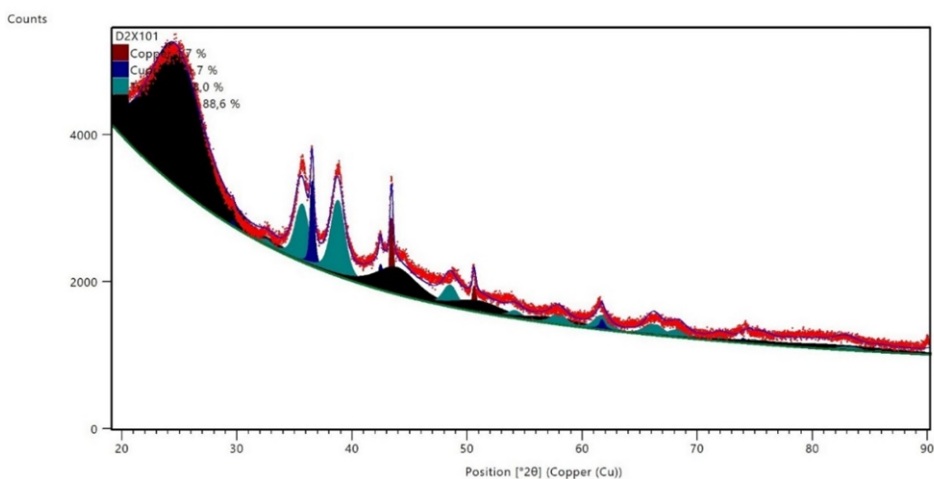
The initial copper synthesis (D2X094-101) were explored using the carbon support (Ketjen Black ec-300). Precursors tested were both copper nitrate ($\text{Cu}(\text{NO}_3)_2$) and copper chloride (CuCl_2). The nitrates have generally been more successful, especially for the Ni experiments, but the D2X071 experiment used $\text{Co}(\text{Cl}_2)$ to great success, so chlorides were included. The effect of glycerol (0 30 Glyc:Cu ratio), and temperature (T_v and $T_{\text{mix}1}$) were also investigated. While the lower temperatures of $T_{\text{mix}1}=250$ °C did not work for Cobalt and Nickel synthesis, Copper has a more positive reduction potential as so it should be easier to reduce. This understanding led to the investigation of the lower temperatures specifically for Cu. The D2X094-101 experiments resulted in Cu loadings well under the intended 20%.

The poor Cu yields in the D2X094-099 experiments suggest more hydrogen needs to be available to provide enough reduction for the intended reaction. Therefore, higher temperatures and higher glycerol amounts were used for D2X100-101. Unfortunately, the D2X101-102 experiments resulted in low Cu loadings again. However, the D2X101 was characterized by a very small Cu particle size, even in carbon. Cu is quite mobile so it is expected that particles agglomerate under the reactors conditions, which would be further exacerbated by the use of carbon black. The small particle size was determined by XRD (Figure 5.1.a), where the fitting of the pattern could not give rise to a crystallite size estimate. This limitation usually occurs in very small and amorphous nanoparticles, and it can be confirmed by SEM analysis (Figure 5.1.b). While SEM will not be able to detect such small particles, EDX will be able to detect a Cu signal.

D2X106-107 were used as control experiments to assess the effect of higher glycerol in D2X100-101. There is still high temperatures to ensure H_2 in the reaction zone, but with less glycerol. These experiments resulted in similarly poor yields, suggesting that too much glycerol is unlikely to interfere with the intended reaction. The particle sizes in D2X100-101 are quite large, suggesting that although glycerol has no effect on the Cu yield, it might still affect the particle size.

A different strategy was implemented by premixing the precursors in experiments D2X103-105, while D2X102 remains a control (eg. precursors not premixed). The understanding from the previous experiments in DTI is that premixing the precursors could better help the metal dispersion on the support, this is due to the mitigation of the laminar flow effect. The supercritical reactor has a laminar flow, by premixing supports and precursors we ensure they react together. Another understanding is that higher flow rates for the precursors will significantly reduce the retention time in the reactor, and therefore yield more homogenous catalyst nanoparticle sizes. Again, the Cu yields did not reach the aimed loading of 20% in these experiments (D2X102-105). When comparing the SEM/EDX data D2X102-103, premixing did not seem to influence Cu loading or dispersion. Flow rates seemed to have little effect on dispersion as well.

(a)



(b)

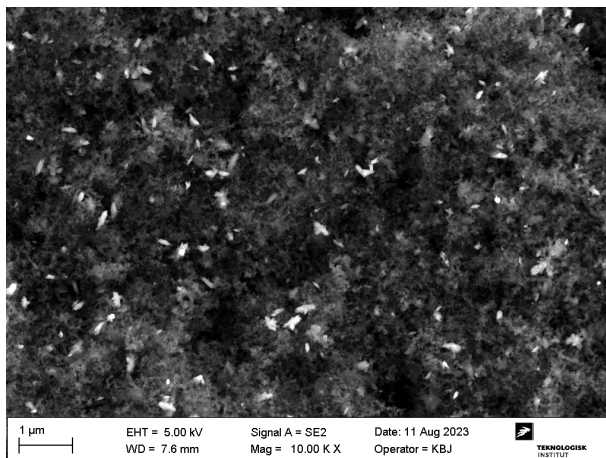


Figure 5.1. XRD analysis (a) and SEM analysis (b) of copper synthesis D2X101 (12.6 wt.% Cu supported on Ketjen Black).

Among the D2X094-107 experiments, the D2X104 had the most promising Cu yield of 16,7 %wt., which is >80% of the aimed Cu loading (20%). Therefore, the D2X104 parameters were used for the upscaled synthesis experiments on Ketjen Black (D2X110-111). D2X110 did not replicate the Cu yield of D2X104, yielding only 21,8 %wt., which is only 65% of the aimed loading (33%). The upscaled synthesis experiments on γ -Al₂O₃ and MgO supports (D2X108, D2X109, and D2X112) used similar experimental parameters as the Nickel experiments: high temperatures and high glycerol. Unlike the Ni experiments, the Cu yields did not meet the aimed yields on the γ -Al₂O₃ support but did meet the aimed yield on the MgO support.

Table 5.1. Summary of synthesis design for the Cu catalysts.

	Cu Precursor	Aimed Loading	Support	Reducing Agent	Ratio (Reducing agent/Cu precursor)	Solvent	Tmix	Tv	P	EDX Cu (%)	Crystallite size (nm)
D2X094	Cu(NO ₃) ₂	20	Carbon Black			ETOH	320	300	300	8.5	39
D2X095	Cu(NO ₃) ₂	20	Carbon Black	glycerol	15	ETOH	320	300	300	13	47
D2X096	CuCl ₂	20	Carbon Black			ETOH	320	300	300	0.2	50
D2X097	CuCl ₂	20	Carbon Black	glycerol	15	ETOH	315	300	300	4.8	50
D2X098	CuCl ₂	20	Carbon Black	glycerol	15	ETOH	250	300	300	5.5	50
D2X099	Cu(NO ₃) ₂	20	Carbon Black	glycerol	15	ETOH	250	300	300	1.8	50
D2X100	CuCl ₂	20	Carbon Black	glycerol	30	ETOH	360	400	300	11.7	50
D2X101	Cu(NO ₃) ₂	20	Carbon Black	glycerol	30	ETOH	360	400	300	12.6	?
D2X102	Cu(NO ₃) ₂	20	Carbon Black	glycerol	15	ETOH	315	400	300	14.6	58
D2X103	Cu(NO ₃) ₂	20	Carbon Black	glycerol	15	ETOH	308	400	300	13.1	56
D2X104	Cu(NO ₃) ₂	20	Carbon Black	glycerol	15	ETOH	308	400	300	16.7	48
D2X105	Cu(NO ₃) ₂	20	Carbon Black	glycerol	15	ETOH	300	400	300	13.7	49
D2X106	CuCl ₂	20	Carbon Black	glycerol	15	ETOH	360	400	300	9	?
D2X107	Cu(NO ₃) ₂	20	Carbon Black	glycerol	15	ETOH	360	400	300	14.7	68
D2X108	Cu(NO ₃) ₂	20	γ-Al ₂ O ₃	glycerol	15	ETOH	360	400	300	14	39
D2X109	Cu(NO ₃) ₂	20	MgO	glycerol	15	ETOH	360	400	300	16.6	
D2X110	Cu(NO ₃) ₂	33	Carbon Black	glycerol	15	ETOH	308	400	300	21.8	
D2X111	Cu(NO ₃) ₂	20	Carbon Black	glycerol	15	ETOH	308	400	300	34.4	
D2X112	Cu(NO ₃) ₂	33	γ-Al ₂ O ₃	glycerol	15	ETOH	308	400	300	19.6	

6. Synthesis of Pt-based catalysts

Pt was selected as a control catalyst sample in efforts to replicate a volcano plot based in literature.³ A 100% ethanol synthesis for platinum catalysts have been established in-house using a Pt(Cl₆) precursor on Carbon black supports. The reduction potentials for metallic platinum are very positive, where the ethanol solvent suffices as a reducing agent. Loadings of 60% and 30% Pt were selected to match the %at. loadings of a typical 20% and 10% of Cobalt or Nickel. D2X115 and D2X116 had aimed loadings of 45% and 30% Pt on a carbon black support, respectively. D2X115 was originally planned to be 60% Pt but a 45% Pt precursor solution was utilized due to human error. This synthesis recipe was also expanded to use the more relevant γ -Al₂O₃ support to give better comparisons. D2X117 and D2X118 had aimed loadings of 60% and 30% Pt on a γ -Al₂O₃ support, respectively. All synthesis yielded their intended aim loadings.

Table 6.1. Summary of synthesis design for the Pt catalysts.

	Pt Precursor	Aimed Loading	Support	Reducing Agent	Ratio (Reducing agent/Pt precursor)	Solvent	Tmix	Tv	P	EDX Pt (%)	Crystallite size (nm)
D2X115	Pt(Cl ₆)	45	Carbon Black	-	-	ETOH	260	200	300	46.8	
D2X116	Pt(Cl ₆)	30	Carbon Black	-	-	ETOH	260	200	300	32.5	
D2X117	Pt(Cl ₆)	60	γ -Al ₂ O ₃	-	-	ETOH	250	200	300	61.3	
D2X118	Pt(Cl ₆)	30	γ -Al ₂ O ₃	-	-	ETOH	250	200	300	34.6	

7. Synthesis of Ru-based catalysts

Ru was selected as the other control catalyst sample in efforts to replicate a volcano plot based in literature.³ It is also of particular interest for comparisons as a state-of-the-art catalyst for the Haber-bosch process. A 100% ethanol synthesis for ruthenium catalysts have been established in-house using a Ru(acac) precursor on Carbon black supports. Loadings of 40% and 40% Ru were selected to match the %at. loadings of a typical 20% and 10% of Cobalt or Nickel. D2X120 and D2X121 had aimed loadings of 40% and 20% Ru on a carbon black support, respectively. This synthesis recipe was also expanded to use the more relevant γ -Al₂O₃ support to give better comparisons. D2X122 and D2X123 had aimed loadings of 40% and 20% Ru on a γ -Al₂O₃ support, respectively. All synthesis yielded their intended aim loadings.

Table 7.1. Summary of synthesis design for the Ru catalysts.

	Ru Precursor	Aimed Loading	Support	Reducing Agent	Ratio (Reducing agent/Ru precursor)	Solvent	Tmix	Tv	P	EDX Ru (%)	Crystallite size (nm)
D2X120	Ru(acac)	40	Carbon Black	-	-	ETOH	300	300	300	37.3	
D2X121	Ru(acac)	20	Carbon Black	-	-	ETOH	300	300	300	21.2	
D2X122	Ru(acac)	40	γ -Al ₂ O ₃	-	-	ETOH	300	300	300	40.3	
D2X123	Ru(acac)	20	γ -Al ₂ O ₃	-	-	ETOH	300	300	300	18.8	

8. Plasma Activities of Co, Ni, Cu, Pt, Ru

Select synthesis samples were sent to UoL to be tested for activity in the plasma reactor. The selection was to test the various quantities of catalyst metal (Co, Ni, Cu, Pt, Ru) loaded on various supports (γ -Al₂O₃, carbon black, MgO). In addition, commercial samples from Riogen were used as references: 5%, 10%, 20% Cobalt or Nickel supported on γ -Al₂O₃, and 10% Cobalt supported on carbon black (Co5, Ni5, Co10, Ni10, Co20, Ni20, and CCo10, respectively). The plasma reactor used a discharge power of 8 W, at a temperature of 110 °C at 1 bar of pressure. The working gas had a N₂:H₂ ratio of 1:3 and a flow rate of 40 ml min⁻¹. The AC power supply used a frequency of 11kHz and a voltage of up to 30 kV. The plasma reactor activity was summarized in terms of ammonia concentration (ppm_{NH₃}) in Figure 8.1.

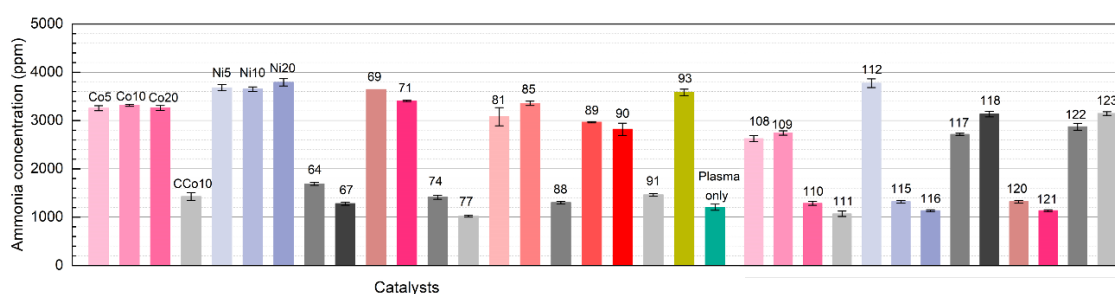


Figure 8.1. Plasma activities of catalyst samples defined by ammonia concentration (ppm_{NH₃}) of the working gas (1:3 N₂:H₂, 40 ml min⁻¹). UoL's plasma reactor (110 °C, 1 bar) used a discharge power of 8 W, with an AC power supply (11 kHz, <30 kV).

All twelve of the samples supported on carbon black had poor activity (D2X64,67,74,77,88,91,110,111,115,116,120,121), including the commercial reference sample (CCo10). This finding remained consistent across all loadings of all catalyst metals tested. The ammonia outputs of these samples were comparable to a reactor without any catalyst at all (plasma only), suggesting that the samples supported on carbon didn't have any catalytic effect on enhancing ammonia output.

There were eighteen samples supported on γ -Al₂O₃, including the six commercial reference samples (Co5, Co10, Co20, Ni5, Ni10, Ni20). Among these reference samples, the nickel-loaded samples had a higher activity than the cobalt-loaded samples (Ni:3600-3800 ppm_{NH₃}, and Co:3200-3400 ppm_{NH₃}, respectively). However, there wasn't a significant difference in activity between the 5%, 10% and 20% loadings of these metals. Among the synthesized samples, the cobalt-loaded samples (D2X69,71) showed higher activity than the nickel-loaded samples (DX81,85,89,90) (Co:3400-3600 ppm_{NH₃}, and Ni:2800-3400 ppm_{NH₃}, respectively). Again there wasn't a significant difference in activity among the various loadings of these metals. However, there was a significant difference in activity among the loadings of copper loaded on γ -Al₂O₃, where a 20% (D2X108) and 33% (D2X112) Cu loading resulted in 2600 and 3800 ppm_{NH₃}, respectively. In addition, Pt- and Ru-loaded samples (D2X117,118,122,123) had the poorest activities (Pt:2700-3200 ppm_{NH₃}, and Ru:2900-3400 ppm_{NH₃}), where the higher loaded samples performed worse. Ni- and Cu-loaded samples on MgO support were also tested, and resulted in similar activities (Ni:3600 ppm_{NH₃}, and Cu:2800 ppm_{NH₃}) to similar samples supported on γ -Al₂O₃.

Literature has suggested that the activity differences between catalyst metals would span several orders of magnitude, where Nickel and Cobalt would be the best.³ While our data can suggest that cobalt and nickel yield the best activities, the activities of our data span 1 order of magnitude. This suggests that the catalyst metal is much less pivotal for the success of competitive ammonia activities than has been thought previously. In addition, the catalyst support showed more notable differences. There are numerous ways a support can affect catalyst activity. The electronegativity of the support can affect the properties of the catalyst metal, thereby indirectly influencing ammonia output. The support surface could also directly be involved in the catalytic reaction, working in conjunction with the catalyst metal surface at the catalyst-support interface. Experimentally, it is difficult to elucidate what exactly is happening when a catalyst support becomes influential to the overall catalyst activity.

9. Catalysts using sorption materials.

An additional investigation is the incorporation of sorption material in the catalyst synthesis (T2.4). Y-zeolite and mordenite were considered promising sorption materials and were therefore tried as a catalyst support for supercritical synthesis. When investigating new support materials, stable dispersions are essential for consistent supercritical synthesis. Previously with Al_2O_3 -based supports, stable dispersions have usually required milling to get an average particle size of $\leq 1.0 \mu\text{m}$. A homogenous size distribution with an average of $\leq 1.0 \mu\text{m}$ was achieved (Figure 9.1), which was preserved for 10+ days in stirring ethanol. Despite these successful millings, the initial flowthrough experiments resulted in only 60% of the expected mass yields. It should be noted that all flowthrough experiments used the same conditions as the Co and Ni synthesis ($T_v=400\text{C}$, $T_{\text{mix}1}=350$, $p=300 \text{ bar}$, 100% EtOH solvent, 100% EtOH precursor solutions).

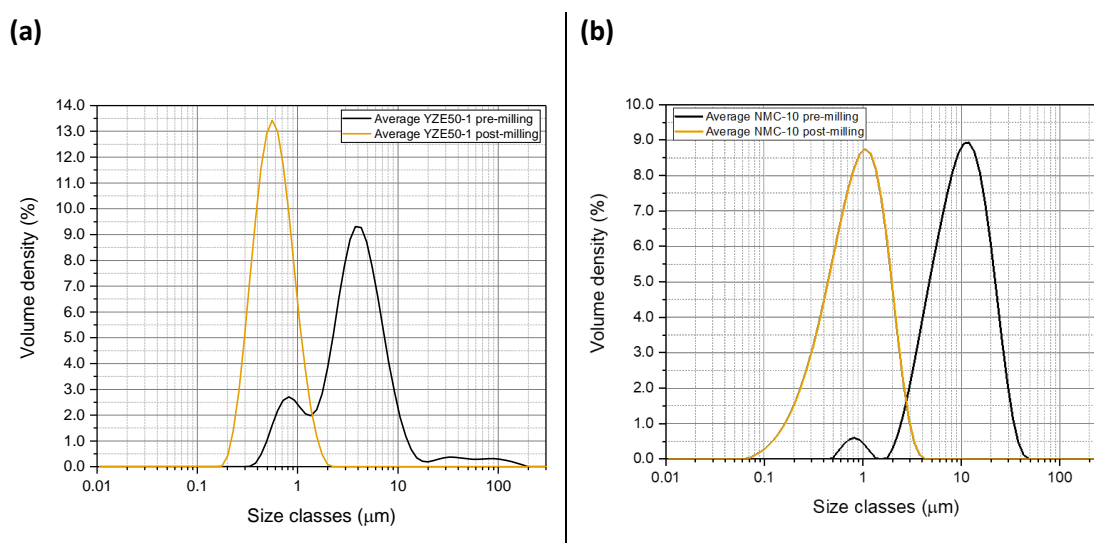


Figure 9.1. Average particle size of γ -zeolite (YZE50-1) and mordenite (NMC-10). Measurements were done before (pre-milling) and after (post-milling) the standard milling procedure to deduce its effects. A Mastersizer 3000 (Malvern) was used for the particle size analysis.

Dispersants/surfactants are typically used to stabilize aqueous dispersions, so Dolapix CE64 (DPX) and Polyethylene glycol 400 (PEG) were utilized based on literature.^{4,5} It was verified that these dispersants do not work in 100% ethanol solutions, but were satisfactory in 5% solutions. The initial flowthrough of 10 %wt. DPX in 95:5 (EtOH:H₂O, %vol.) proved successful with a 92% mass yield (Figure 9.2a, green). However, when adding the necessary glycerol, the mass yield went down to 62% (Figure 9.2a, red).

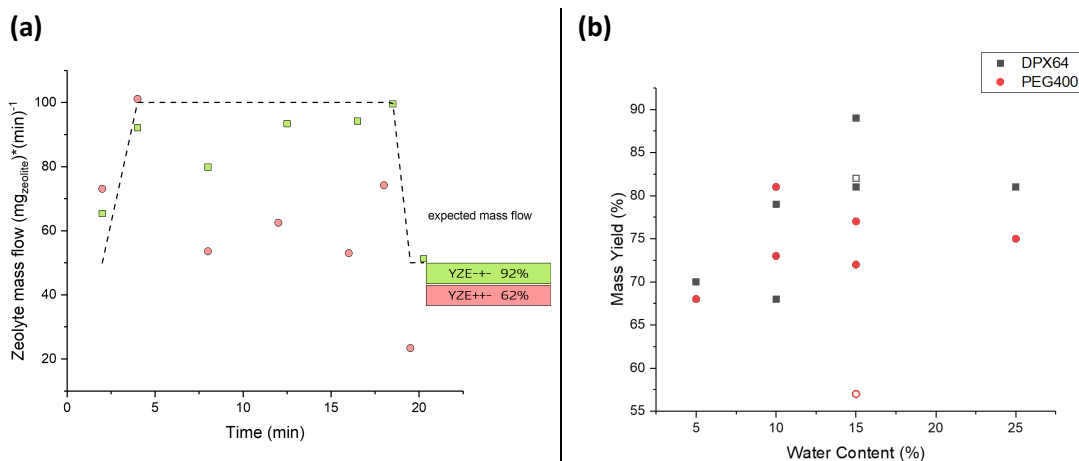


Figure 9.2. (a) Y-zeolite flowthrough analysis measuring the zeolite mass flow ($\text{mg}_{\text{zeolite}} \cdot \text{min}^{-1}$) of timed-interval batches (min). Y-zeolite dispersions (2g) were with (YZE+- red) or without (YZE+-) glycerol. Dashed line is an expected mass flow (100% mass yield). (b) Mass yields of flowthrough analysis of γ -zeolite dispersions with varying water content (5-25 %vol.), dispersant type (DPX64, PEG400), and dispersant concentration (solid: 10 %wt., hollow: 1 %wt.). Supercritical flow reactor parameters for all experiments (D2X130-143): $T_v=400$ °C, $T_{\text{mix1}}=350$ °C, $p=300$ bar, 100% EtOH solvent, 75-95% EtOH precursor solutions.

Optimizing the zeolite dispersion in the presence of glycerol was then extensively studied (Figure 9.2b). A water content of 15 %vol. and a DPX content 1 %wt. resulted in a mass yield of >80%. (D2X142). While higher water contents could have possibly resulted in better yields, it could also potentially be problematic for the reaction. Therefore, the D2X142 parameters were used for the catalyst synthesis supported on YZE.

Table 9.1. Summary of flow through analysis experiments using γ -zeolite dispersions in EtOH with varying water content (5-25 %vol.), dispersant type (DPX64, PEG400), and dispersant concentration (%wt.). Supercritical flow reactor parameters for all experiments (D2X130-143): $T_v=400$ °C, $T_{mix1}=350$ °C, $p=300$ bar, 100% EtOH solvent, 75-95% EtOH precursor solutions.

	Support	Dispersant	Dispersant (%wt.)	Water (%vol.)
D2X130	Y Zeolite	Dolapix	10	5
D2X131	Y Zeolite	PEG	10	5
D2X132	Y Zeolite	Dolapix	10	10
D2X133	Y Zeolite	PEG	10	10
D2X134	Y Zeolite	Dolapix	10	15
D2X135	Y Zeolite	PEG	10	15
D2X136	Y Zeolite	Dolapix	10	25
D2X137	Y Zeolite	PEG	10	25
D2X138	Y Zeolite	Dolapix	10	10
D2X139	Y Zeolite	PEG	10	10
D2X140	Y Zeolite	Dolapix	10	15
D2X141	Y Zeolite	PEG	10	15
D2X142	Y Zeolite	Dolapix	1	15
D2X143	Y Zeolite	PEG	1	10

Synthesis using γ -zeolite supports had aimed loadings of 1-5 %wt. using nickel or cobalt. Initial experiments with the unoptimized dispersions were conducted, where D2X126 and D2X127 had mass yields of 59% and 62% respectively. Subsequent experiments (D2X149, D2X150, D2X151, D2X152) used the optimized dispersion parameters from D2X142, but the mass yields were not consistently better. The efficacy of this dispersion is likely limited to before reaching the supercritical zone of the reactor, where the dispersion will be compromised in supercritical conditions.

Premixing the catalyst precursors with the zeolite support was therefore considered, in order to have better control over the mass yield and loading. D2X155 and D2X156 yielded better mass yields (74% and 71% respectively), but the lower aimed catalyst loadings might be partially responsible for these results.

Table 9.2. Summary of nickel and cobalt catalysts supported on γ -zeolite. D2X148-156 used the dispersion parameters from D2X142. Supercritical flow reactor parameters for all experiments: $T_v=400$ °C, $T_{mix1}=350$ °C, $p=300$ bar, 100% EtOH solvent, 75-95% EtOH precursor solutions.

Sample	Co (wt.%)	Ni (wt.%)	Support	Mass yield (%)	Comment
D2X126	-	6,3 ($\pm 0,1$)	YZE	59	unoptimized dispersion
D2X127	6,0 ($\pm 0,1$)	-	YZE	62	unoptimized dispersion
D2X148	-	-	YZE	61	Flowthrough Optimized dispersion
D2X149	-	6,7 ($\pm 0,5$)	YZE	57	Optimized dispersion
D2X150	5,8 ($\pm 0,1$)	-	YZE	73	Optimized dispersion
D2X151	1,5 ($\pm 0,0$)	-	YZE	54	Optimized dispersion
D2X152	-	1,4 ($\pm 0,0$)	YZE	63	Optimized dispersion
D2X155	2,2 ($\pm 0,7$)	-	YZE	74	Optimized dispersion Co+YZE premixed
D2X156	-	1,6 ($\pm 0,1$)	YZE	71	Optimized dispersion Ni+YZE premixed

Additional syntheses were explored using YZE support. Iron (D2X169) and iron alloys (D2X170-171) were tested to explore the effect of iron alloys with the state-of-the-art Ni and Co catalysts. In addition, the ion-exchange method (instead of SCF synthesis) was used to synthesize D2X185-187. This alternative synthesis method was used by UoL, and we reproduced their synthesis to determine if any clear advantages of the SCF reactor synthesis are justifying the extra efforts. In addition, Mo was attempted because it was screened as a potential candidate by NIC. However, the Mo precursors had solubility issues for the SFC method and was completely ineffective for the ion-exchange method, as evidenced by the EDX results of D2X182, which had an aimed Mo loading of 5 (wt.%).

Table 9.3. Summary of the iron and iron-alloy catalysts (D2X169-171, SCF method) and Mo (D2X182), Co (D2X183), Ni (D2X184), catalysts (ion-exchange method) supported on γ -zeolite. Supercritical flow reactor (SCF) parameters for relevant experiments: $T_v=400$ °C, $T_{mix1}=350$ °C, $p=300$ bar, 100% EtOH solvent, 85% EtOH precursor solutions. The standard ion-exchange method was used for relevant experiments (refer to Section 12).

Sample	Co (wt.%)	Ni (wt.%)	Fe (wt.%)	Mo (wt.%)	Support	Method
D2X169	-	-	1,0 ($\pm 0,2$)	-	YZE	SCF
D2X170	-	0,6 ($\pm 0,1$)	0,7 ($\pm 0,0$)	-	YZE	SCF
D2X171	0,5 ($\pm 0,0$)	-	0,6 ($\pm 0,1$)	-	YZE	SCF
D2X182	-	-	-	-	YZE	Ion-Exchange
D2X183	6,6	-	-	-	YZE	Ion-Exchange
D2X184	-	6,1	-	-	YZE	Ion-Exchange

The catalysts supported on γ -zeolite were ultimately underwhelming. Plasma reactor performance of D2X126-127,148-152,155-156 were all below 3000 ppm_{NH₃}. The D2X148 sample was a support sample without any catalyst and yielded only ~1900 ppm_{NH₃}, while an empty reactor without any sample yields ~1200 ppm_{NH₃}. This suggests that the actual catalyst effect is a minor fraction of the actual activity. Additionally, the iron (D2X169) and iron alloys (D2X170-171) performed worse (<2400 ppm_{NH₃}) than the Ni or Co samples of comparable loadings (D2X151,152,155,156). In addition, the ion-exchange method samples (D2X182-184: 1800-2600 ppm_{NH₃}) were slightly worse in performance to the SFC samples of similar loading (D2X126,127,149,150: 2600-3000 ppm_{NH₃}). Synthesis experiments (D2X187<) focused more on ion exchange and wetness impregnation methods.

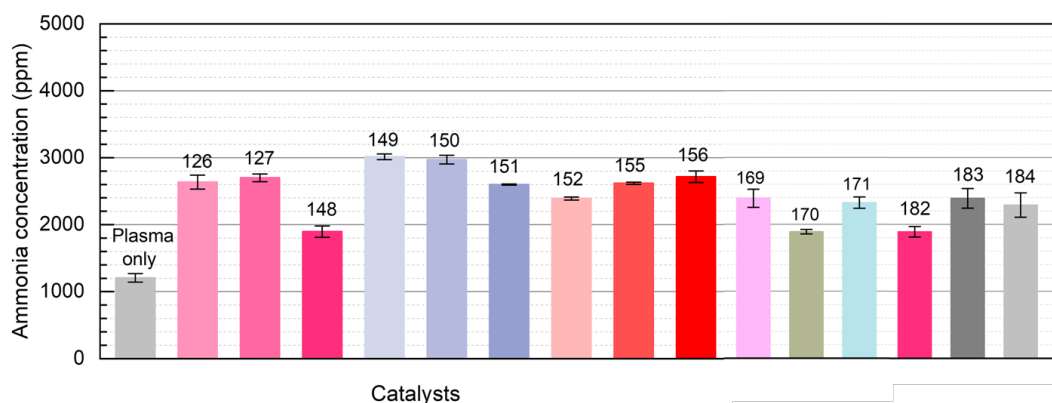


Figure 9.3. Plasma activities of catalyst samples defined by ammonia concentration (ppm_{NH₃}) of the working gas (1:3 N₂:H₂, 40 ml min⁻¹). UoL's plasma reactor (110 °C, 1 bar) used a discharge power of 8 W, with an AC power supply (11 kHz, <30 kV).

10. Synthesis of catalyst alloys with promoters.

University of Liverpool (UoL) had good plasma catalytic performances using samples supported on 5A, which inherently contains 7 %wt. calcium, a suspected promoter. We investigated doping YZE with a promoter (Ca or Ba) to see if this would have a similar effect (Task 2.3). Two routes were investigated for implementing promoters to the YZE support, a simple premixing procedure, and a more extensive calcining procedure (Figure 8.1). The calcining procedure involved mixing the YZE support with a concentration of BaOH or CaOH overnight. The aqueous solvent was then removed by evaporation, and the obtained powder was calcined to 700 °C for 5 h in static air.

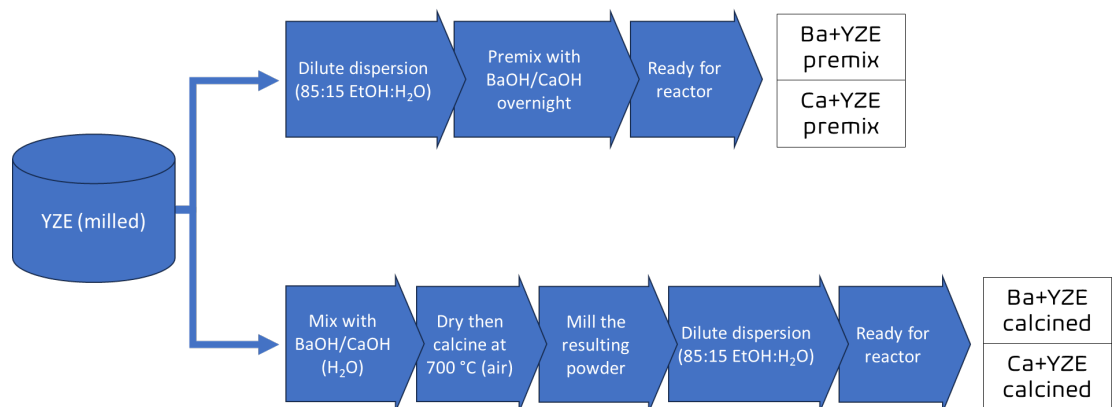


Figure 10.1. Scheme summarizing the two strategies used to implement promoter (Ba or Ca) to SCF synthesis.

As a starting point, the molar ratio between the catalyst and promoter was estimated to be between 5-10:1 (catalyst:promoter). D2X157 and D2X158 used a premixed barium YZE support, while D2X163 and D2X164 used premixed calcium YZE support. D2X159 and D2X162 used a calcined barium YZE support with an aimed promoter loading of 0.01 wt.%, while D2X160 and D2X162 used a calcined barium YZE support with an aimed promoter loading of 0.1 wt.%. D2X165 and D2X168 used a calcined calcium YZE support with an aimed promoter loading of 0.03 wt.%, while D2X166 and D2X167 used a calcined calcium YZE support with an aimed promoter loading of 0.3 wt.%.

Table 10.1. EDX analysis of nickel and cobalt catalysts supported on promoted γ -zeolite. Supercritical flow reactor parameters for all experiments: $T_v=400$ °C, $T_{mix1}=350$ °C, $p=300$ bar, 100% EtOH solvent, 85% EtOH precursor solutions.

	Co (wt.%)	Ni (wt.%)	Ba (wt.%)	Ca (wt.%)	Support	Comment
D2X157	1,6 ($\pm 0,0$)	-	0,3 ($\pm 0,1$)	-	YZE	Ba+YZE premixed
D2X158	-	1,5 ($\pm 0,1$)	0,2 ($\pm 0,1$)	-	YZE	Ba+YZE premixed
D2X159	1,2 ($\pm 0,1$)	-	0,0 ₇ ($\pm 0,1$)	-	YZE	Ba+YZE calcined
D2X160	1,5 ($\pm 0,0$)	-	1,6 ($\pm 0,0$)	-	YZE	Ba+YZE calcined
D2X161	5,3 ($\pm 0,8$)	-	1,4 ($\pm 0,2$)	-	YZE	Ba+YZE calcined
D2X162	0,3 ($\pm 0,0$)	1,5 ($\pm 0,1$)	0,2 ($\pm 0,0$)	-	YZE	Ba+YZE calcined
D2X163	1,4 ($\pm 0,2$)	-	-	0,0 ₇ ($\pm 0,0_6$)	YZE	Ca+YZE premixed
D2X164	-	1,3 ($\pm 0,0$)	-	0,0 ₇ ($\pm 0,0_6$)	YZE	Ca+YZE premixed
D2X165	1,8 ($\pm 0,1$)	-	-	0,0 ₃ ($\pm 0,0_5$)	YZE	Ca+YZE calcined
D2X166	1,4 ($\pm 0,1$)	-	-	0,3 ($\pm 0,0$)	YZE	Ca+YZE calcined
D2X167	5,6 ($\pm 0,2$)	-	-	0,3 ($\pm 0,0$)	YZE	Ca+YZE calcined
D2X168	-	1,3 ($\pm 0,0$)	-	0,1 ($\pm 0,0$)	YZE	Ca+YZE calcined

Additional synthesis were explored using promoted YZE support. NiFe (D2X176, D2X179), CoNi (D2X177, D2X180) and CoFe (D2X178, D2X181) alloys were tested in combination with a promoter of either Ba (D2X176-178) or Ca (D2X179-181).

Table 10.2. EDX analysis of bimetallic catalysts supported on promoted γ -zeolite. Supercritical flow reactor parameters for all experiments: $T_v=400$ °C, $T_{mix1}=350$ °C, $p=300$ bar, 100% EtOH solvent, 85% EtOH precursor solutions.

	Co (wt.%)	Ni (wt.%)	Fe (wt.%)	Ba (wt.%)	Ca (wt.%)	Support	Comment
D2X176	-	1,0 ($\pm 0,0$)	0,5 ($\pm 0,0$)	0,8 ($\pm 0,0$)	-	YZE	Ba+YZE premixed
D2X177	1,2 ($\pm 0,1$)	1,2 ($\pm 0,1$)	-	0,8 ($\pm 0,0$)	-	YZE	Ba+YZE premixed
D2X178	1,1 ($\pm 0,1$)	-	1,3 ($\pm 0,2$)	0,7 ($\pm 0,0$)	-	YZE	Ba+YZE premixed
D2X179	-	0,9 ($\pm 0,0$)	0,5 ($\pm 0,0$)	-	1,5 ($\pm 0,0$)	YZE	Ca+YZE premixed
D2X180	0,9 ($\pm 0,1$)	0,9 ($\pm 0,1$)	-	-	1,3 ($\pm 0,1$)	YZE	Ca+YZE premixed
D2X181	1,1 ($\pm 0,1$)	-	0,7 ($\pm 0,1$)	-	1,5 ($\pm 0,0$)	YZE	Ca+YZE premixed

The results of D2X157-168 and D2X176-181 were unremarkable (2600-3500 ppm_{NH3}). This suggests that the promoters do not work with the γ -zeolite support in the same way as zeolite 5A. The samples with higher catalyst loading (D2X161 and D2X167) have the most activity, suggesting a catalytic effect on activity, albeit very modest.

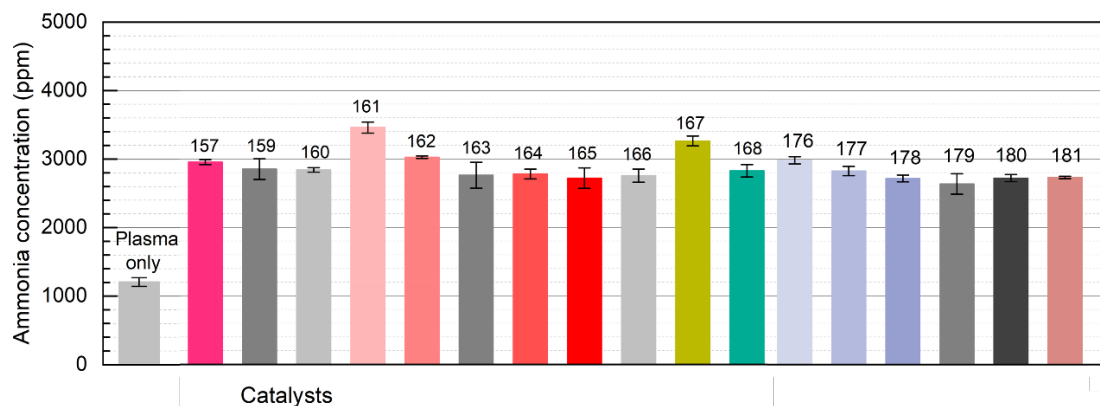


Figure 10.2. Plasma activities of catalyst samples defined by ammonia concentration (ppm_{NH3}) of the working gas (1:3 N₂:H₂, 40 ml min⁻¹). UoL's plasma reactor (110 °C, 1 bar) used a discharge power of 8 W, with an AC power supply (11 kHz, <30 kV).

11. Synthesis of single atom and cluster catalysts.

The cluster and single-atom synthesis (Task 2.1) were explored using cobalt. We used cobalt for these experiments because we found relevant methods in the literature.^{6,7} These methods are based on sol gel reactions, where the zeolite forms and encapsulates chelated cobalt species in order to control their particle size. These chelators are organic ligands that will be burned away during the final calcination step used to crystallize the zeolites.

The cluster synthesis involved chelating the cobalt with ligands (EDA or TPE) and then sequentially adding the precursors for the zeolite via a sol gel reaction.⁶ Syntheses with chelating ligands involved the initial dropwise addition of aqueous $\text{CoCl}_2 \cdot 6\text{H}_2\text{O}$ (0.18–0.91 g in 9 ml H_2O) at a rate of (0.2 $\text{cm}^3 \text{ s}^{-1}$) to aqueous ligand solutions (0.09–1.39 cm^3 9 ml H_2O) while stirring (ligand/metal molar ratios between 1-3). The aqueous solutions of ligands and metal cations were then transferred into 125 ml polypropylene bottles, and colloidal silica (5.3 g, Ludox AS-30) and NaOH (2.4 g) were sequentially added. The containers were sealed and kept at 353 K for 0.5 h with stirring and then cooled to ambient temperature. Aqueous NaAlO_2 (3.0 g in 9 ml H_2O) was then added, and stirred for 2 h at ambient temperature. The resulting homogeneous synthesis gels contained molar ratios of 1.7 $\text{SiO}_2/1 \text{ Al}_2\text{O}_3/3.2 \text{ Na}_2\text{O}/110 \text{ H}_2\text{O}/0.066\text{--}0.33 \text{ Co}/0.066\text{--}0.99$ ligand.

Table 11.1. Summary of the sol gel reactants for the cluster synthesis samples.

	D2X172	D2X173
Chemical	Mass (g)	Mass (g)
CoCl_2	0,5	1,0
EDA	1,6	0
TPE	0	1,0
NaAlO_2	3,0	3,0
SiO_2	6,3	6,8
NaOH	2,4	2,4

The bottles containing the gels were sealed and the contents heated to 373 K for 12 h while stirring to form as-synthesized CoNaLTA samples. The solids formed were separated centrifugation and washed with deionized water until the rinse liquids reached a pH of 7–8. They were then treated in a convection oven at 373 K for 8 h. The solids were finally heated in flowing dry air ($1.67 \text{ ml g}^{-1} \text{ s}^{-1}$) from ambient to 623 K (at 0.033 K s^{-1}) and held for 3 h. The resulting powders had Si:Al ratios of $\sim 1:1$, which was expected of an LTA sample. D2X172 had higher loadings and the powder was inhomogeneous, suggesting inadequate chelation and/or rinsing of the cobalt species. D2X173 resulted in a homogenous powder with the expected Co loading of 1,0 (at. %), repeating the literature findings of using TPE as a chelator.⁶

Table 11.2. EDX analysis of the cluster synthesis and single atom synthesis samples.

at.%	C	O	Na	Al	Si	Co
D2X172	4,8	45,5	13,9	16,6	15,4	2,7
D2X173	6,4	56,4	11,0	12,1	13,2	1,0
D2X174	7,3	57,2	9,0	9,6	16,8	0,1
D2X175	8,6	56,1	7,9	9,6	17,3	0,1

A directing agent solution was prepared beforehand and used for the single-atom synthesis.⁷ This directing agent solution is aged for 3 days at room temperature, and is therefore likely a semi-crystallized gel to act as ‘scaffolding’ that the subsequent single-atom sol-gel reaction builds upon. Synthesis of directing agent solution started with mixing NaOH, NaAlO₂, and D.I. water and stirring until the solution is clear. 30 % wt. colloidal silica was then dropwise added to the solution, follow by continuous stirring for 4 h. Lastly, the mixture is aged for 3 days at room temperature.

Single atom synthesis was prepared by mixing CoCl₂ with excess EDA in D.I. water until the solution was clear. NaOH, NaAlO₂, SiO₂, and Directing Agent Solution were added to the aqueous solution successively and continuously stirred for 4 h, then aged at room temperature for 4 h. The reaction mixture was then transferred into a Teflon-lined stainless steel autoclave, and the crystallization was conducted in a conventional oven at 100 °C for 12 h. The as-synthesized solid products were centrifuged, washed with water and ethanol for several times to remove excess Co-EDA complex, and then dried at 80 °C in a vacuum oven overnight. Lastly, the obtained product was calcined in static air at 400 °C for 2 h and reduced in flowing H₂ (5%, 100 ml*min⁻¹*g⁻¹) at 200 °C for 1 h. The resulting powders had Si:Al ratios of ~2,5:1, which was expected of a γ -zeolite sample. The detected cobalt loadings were very low (<1,0 %wt.), and therefore difficult to quantify with EDX.

Table 11.3. Summary of the sol gel reactants for the single atom synthesis samples.

	Directing Agent	D2X174	D2X175
Chemical	Mass (g)	Mass (g)	Mass (g)
CoCl ₂	-	0,13	0,05
EDA	-	3,0	2,0
H ₂ O	50	18,0	18,0
NaAlO ₂	1,7	3,0	1,5
SiO ₂	11,1	8,4	3,3
NaOH	14,2	1,4	0,8
Directing Agent		16,0	16,0

Samples D2X173-175 were tested for plasma activities, and had very poor activities (D2X173-174: 2200 ppm_{NH₃}, D2X175: 1400 ppm_{NH₃}). Very little catalytic effect is observed (if at all), despite the intensive synthesis process. It was therefore not explored further.

12. Zeolites 5A and promoted 4A.

UoL's initial investigations showed that zeolite 5A yielded the best activities (Co_3O_4 -5A: 7500 ppm_{NH_3} , NiO-5A: 6000 ppm_{NH_3}). Zeolite 5A's elemental composition inherently includes calcium (7 %wt.), which is a known promoter. In addition, UoL tested a Ca-doped 4A support without catalyst with promising activities (4A+Ca: 3500 ppm_{NH_3} , 4A: 900 ppm_{NH_3} , 5A: 3300 ppm_{NH_3}). Stable dispersions of adequate concentrations of 4A and 5A were not realized, and therefore the supercritical flow reactor was not considered.

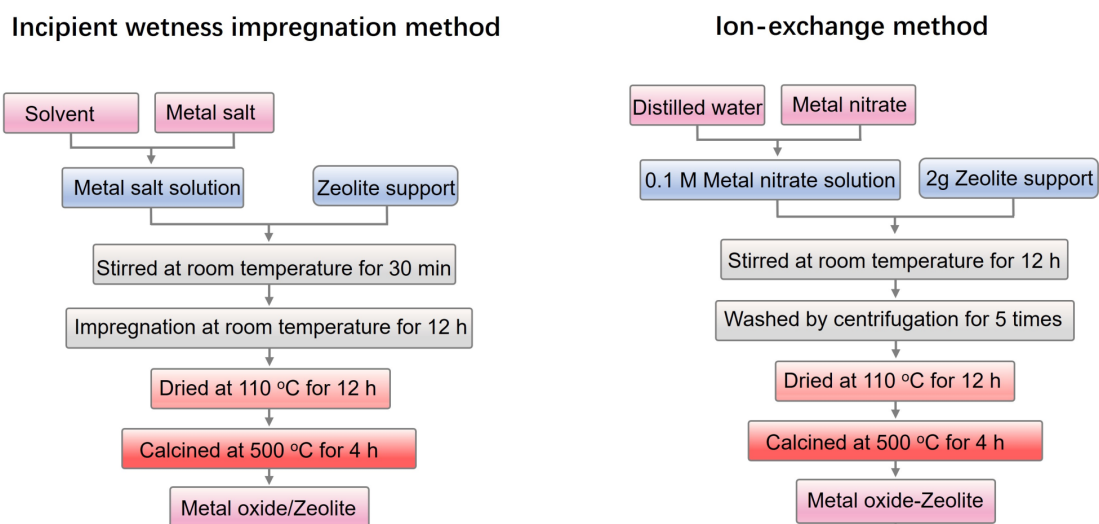


Figure 12.1. Summary of incipient wetness impregnation method and ion-exchange method.

Wetness impregnation and ion exchange methods were therefore explored (Figure 12.1). In a standard wetness impregnation method, 2 ml of metal nitrate salt solution is added to a heated crucible (90 °C) containing 2g of zeolite support and hand-stirred for 10 minutes. The crucible then sits overnight (25 °C, 12 h), then dried (110 °C, 12 h), and then calcined (500 °C, 4 h). In a standard ion-exchange method, 50 ml of metal nitrate salt solution (0.1 M) is stirred with 2 g zeolite support (25 °C, 12 h), and then washed by centrifugation 5 times. The resulting powder is added to a crucible to be dried (110 °C, 12 h), and then calcined (500 °C, 4 h).

Table 12.1. EDX analysis of the initial samples using the ion-exchange method.

Sample	Co (wt.%)	Ni (wt.%)	Fe (wt.%)	Mo (wt.%)	Support	Method
D2X185	-	-	-	12,9 (±0,6)	5A	Ion-Exchange
D2X186	7,3 (±0,3)	-	-	-	5A	Ion-Exchange
D2X187	-	7,2 (±0,3)	-	-	5A	Ion-Exchange

D2X185-187 were initial experiments to replicate the results of UoL that used wetness impregnation on a 5A support. These samples were among the best synthesized (D2X185: 2800 ppm_{NH_3} , D2X186: 3500 ppm_{NH_3} , D2X187: 3700 ppm_{NH_3}), but did not reproduce the success of UoL's samples (6000-7500 ppm_{NH_3}).

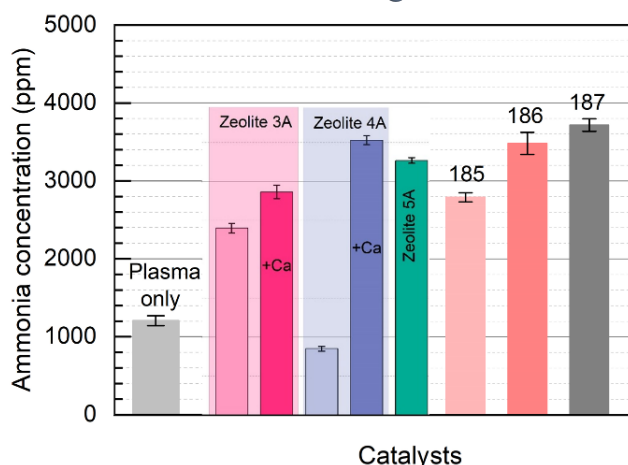


Figure 12.2. Plasma activities of catalyst samples defined by ammonia concentration (ppm_{NH_3}) of the working gas (1:3 $\text{N}_2:\text{H}_2$, 40 ml min^{-1}). UoL's plasma reactor (110°C , 1 bar) used a discharge power of 8 W, with an AC power supply (11 kHz, <30 kV).

Ba and La are suspected promoters for NH_3 production, particularly with Co and Ni. Therefore, the next investigations were with promoted 4A supports (D2X188-203, 208-210). This involved Ni, NiCo, or NiFe catalysts (5 wt.%) with Ca, Ba, or La promoters (1-20 wt.%). It was apparent that La was not compatible with the ion exchange method (D2X193, 198) because the actual loading was much lower than the aimed loading. Similarly, Ba had some difficulties with the wetness impregnation method, but not as severe. It was generally noted that an actual exchange of ions was not achieved because the bulk Na remained roughly the same (Table 12.2). Since 5A's Ca is a bulk concentration (7-10 wt.%), it seemed reasonable to aim for lower surface concentrations of promoters (1-2 wt.%) in future experiments.

Samples were sent to UoL to be tested (Figure 12.3). D2X194-197 and D2X208-210 had 5 wt. Ni but with different types of promoter (Ca, Ba, La) and loading (1 wt.%, 10 wt.%). In addition, samples with 10% wt. promoter (Ba, La) but without Ni catalyst were also included (D2X198-199). The La samples showed poor activity (D2X194: $2400 \text{ ppm}_{\text{NH}_3}$, D2X195: $2100 \text{ ppm}_{\text{NH}_3}$). The Ba samples showed poor activity (D2X196: $2100 \text{ ppm}_{\text{NH}_3}$, D2X195: $1950 \text{ ppm}_{\text{NH}_3}$). The Ca samples showed poor activity (D2X208: $1700 \text{ ppm}_{\text{NH}_3}$, D2X209: $2700 \text{ ppm}_{\text{NH}_3}$). The unpromoted sample showed the best activity but was still poor (D2X210: $3200 \text{ ppm}_{\text{NH}_3}$). The samples without Ni catalyst also showed poor activity (D2X198: $2800 \text{ ppm}_{\text{NH}_3}$, D2X199: $2600 \text{ ppm}_{\text{NH}_3}$).

Table 12.2. EDX analysis of the samples using the wetness impregnation method (2g batches).

at. %	Na	Al	Si	Ca	Co	Fe	Ni	Ba	La	Comments
4A _{Pegasus}	13,0	13,9	13,2	-	-	-	-	-	-	
D2X188	11,8	12,5	11,7	-	-	-	1,8	2,0	-	4A support
D2X189	12,1	12,7	12,2	-	-	-	2,2	0,3	-	4A support
D2X190	12,3	11,4	10,8	-	0,8	-	1,0	2,0	-	4A support
D2X191	12,2	12,5	11,9	-	0,9	-	0,9	0,3	-	4A support
D2X192	6,8	14,5	13,6	-	-	-	-	5,1	-	4A support
D2X193	12,0	14,0	13,3	-	-	-	-	-	0,5	4A support
D2X194	11,7	12,3	11,7	-	-	-	2,0	-	1,6	4A support
D2X195	12,4	12,9	12,4	-	-	-	2,0	-	0,2	4A support
D2X196	12,1	12,5	11,9	-	-	-	1,7	1,0	-	4A support
D2X197	12,6	12,8	12,3	-	-	-	1,9	0,3	-	4A support
D2X198	10,3	14,2	13,4	-	-	-	-	2,0	-	4A support
D2X199	12,0	14,1	13,4	-	-	-	-	-	0,6	4A support
D2X200	11,7	12,6	11,9	-	-	1,2	1,4	-	0,6	4A support
D2X201	12,5	11,6	11,2	-	-	-	3,0	-	0,8	4A support
D2X202	10,6	12,7	12,0	-	-	1,3	1,4	1,5	-	4A support
D2X203	9,7	12,9	12,4	-	-	-	2,6	1,7	-	4A support
D2X208	12,7	11,9	11,5	0,6	-	-	2,2	-	-	4A support
D2X209	9,5	10,3	9,8	3,9	-	-	1,7	-	-	4A support
D2X210	12,3	12,8	12,3	-	-	-	2,6	-	-	4A support

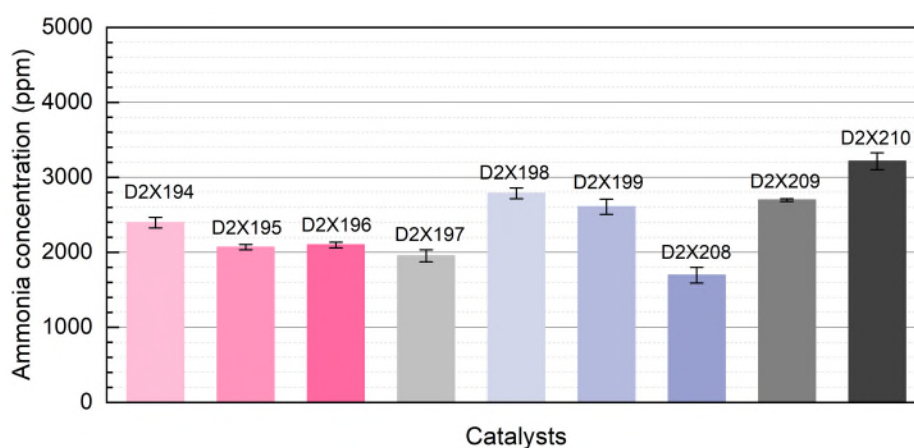


Figure 12.3. Plasma activities of catalyst samples defined by ammonia concentration (ppm_{NH_3}) of the working gas ($1:3 \text{ N}_2:\text{H}_2$, 40 ml min^{-1}). UoL's plasma reactor ($110 \text{ }^\circ\text{C}$, 1 bar) used a discharge power of 8 W , with an AC power supply (11 kHz , $<30 \text{ kV}$).

13. Upscaled synthesis

The wetness impregnation method described in section 12 (Figure 12.1) was upscaled to 10-100g. In a standard upscaled wetness impregnation method, 100 ml of metal nitrate salt solution is added to a 1 L glass bottle containing 1kg milling balls (5mm, zirconia). Then 100g of zeolite support is added and milled for 1-2 hours. The crucible then sits overnight (25 °C, 12 h), then dried (110 °C, 12 h), and then calcined (500 °C, 4 h). The final powder is then sifted to separate from the milling balls. Initial upscaled synthesis (D2X204-207) started with 10g batches and used 5A support so that promoter wouldn't need to be included in the metal nitrate salt solution.

Table 13.1. EDX analysis of the initial samples using the upscaled wetness impregnation method (10g batches).

at. %	Na	Al	Si	Ca	Co	Fe	Ni	Ba	La	Comments
5A _{Pegasus}	3,5	13,8	13,1	5,8	-	-	-	-	-	
D2X204	3,3	13,5	12,8	5,1	-	0,9	1,0	-	-	5A support
D2X205	3,2	13,8	13,2	5,2	-	-	1,9	-	-	5A support
D2X206	3,6	13,1	12,5	5,8	-	1,0	1,0	-	-	5A support
D2X207	3,3	13,5	12,9	5,6	1,0	-	1,1	-	-	5A support

The next synthesis batches (D2X211-217) were scaled up to 50-100g using 4A support, this meant that promoter was included in the metal nitrate salt solution. While the experiments using Ni or NiFe catalyst resulted in homogeneous powders to the naked eye, the experiments using NiCo catalyst did not. This was speculated to occur during the drying phase, where the metal nitrate salts would pool at the top and completely compromise metal dispersion. The D2X214-216 investigated using centrifugation instead. D2X214 (100g) was split into D2X214.1 (50g) and D2X214.2 (50g), where D2X214.1 would follow the standard upscaled wetness impregnation procedure. In D2X214.2, after the zeolite was milled for 1-2 hours, the slurry was sifted and centrifuged once with D.I. water. It was then transferred to a crucible overnight, (25 °C, 12 h), then dried (110 °C, 12 h), and then calcined (500 °C, 4 h). Despite these extra steps, D2X214.2 did not result in a homogenous powder, but it did look better. Noticeably less nickel was detected in D2X214.2 compared to D2X214.1, that is likely lost from the centrifugation step. This investigation was repeated with D2X215-216 to investigate the effect with calcium promoter (D2X216), and also to see if a noticeable improvement was noticed with NiFe catalyst (D2X215). There wasn't any noticeable difference between the homogeneity of D2X215.1 and D2X215.2, but D2X215.2 again had less Nickel detected. The (D2X216) NiCo batch again yielded an inhomogeneous sample, suggesting that the type of promoter isn't responsible for this phenomenon. An additional strategy was used for D2X217, where citric acid was added to the metal nitrate salt solution as a chelator to form the less soluble metal citrates. This was combined with the centrifugation strategy, but the homogeneity of the resulting powder did not improve.

Table 13.2. EDX analysis of the samples using the upscaled wetness impregnation method (50-100g batches).

at. %	Na	Al	Si	Ca	Co	Fe	Ni	Ba	La
4A _{Pegasus}	13,0	13,9	13,2	-	-	-	-	-	-
D2X211	11,6	12,9	12,5	1,1	-	-	0,5	-	-
D2X212	12,0	12,3	11,9	-	-	-	2,2	-	0,2
D2X213	11,7	12,5	12,2	-	1,2	-	1,3	-	0,2
D2X214.1	11,4	13,5	13,2	-	1,3	-	1,3	-	0,3
D2X214.2	10,8	13,7	13,3	-	1,3	-	0,8	-	0,3
D2X214.3	10,5	13,8	13,3	-	1,4	-	0,8	-	0,3
D2X215.1	12,6	11,8	11,6	0,6	-	1,2	1,3	-	-
D2X215.2	10,0	13,9	13,5	0,7	-	1,0	0,7	-	-
D2X216.1	11,5	12,4	12,1	0,6	1,1	-	1,2	-	-
D2X216.2	9,8	13,7	13,2	0,7	1,1	-	1,0	-	-
D2X217	9,7	13,3	14,7	0,6	1,0	-	0,6	-	-

14. Conclusion

Work Package 2 (WP2) was summarized by 4 main objectives: optimize low-CRM catalyst for plasma reactor (OBJ2.1), increase NH_3 synthesis performance by incorporating sorption material into catalyst structure (OBJ2.2), improve catalyst activity with promoters (OBJ2.3), and upscale catalyst production for validation reactors (OBJ2.4). WP2 was split into 5 main tasks (T2.1-2.5).

Task 2.1 focused on the synthesis and test of catalytic structures for plasma catalysis. This focused on benchmarking cobalt-based catalysts (Section 3) and nickel-based catalysts (Section 4). These were compared to copper-based catalysts (Section 5), platinum-based catalysts (Section 6), and ruthenium-based catalysts (Section 7) to complete a volcano plot. Task 2.1 then focused on alloy combinations with other transition metals (mainly iron) to further improve activity and reduce CRM use. This was explored in the subsequent experiments throughout other investigations (Section 9, 10, 12, 13). Finally, Task 2.1 focused on nanoclusters and single-atom catalysts as an alternative to typical nanoparticle catalysts. Sol-gel methods were used to synthesize cobalt clusters and cobalt single atoms (Section 11). Task 2.2 focused on the rational design of catalysts for the plasma reactor. A screening study was implemented to identify promising catalysts (Section 2). The new catalyst candidates such as Fe and Mo were subsequently synthesized and tested (Section 9, 12). Task 2.3 focused on improving catalyst performances with promoters. This was initially achieved by the use of zeolite 5A support, which contained calcium inherently. Calcium and barium promoters were implemented on γ -zeolite support to improve in plasma activity (Section 10). Calcium, barium and lanthanum promoters were implemented on zeolite 4A to improve plasma activity (Section 12). Task 2.4 focused on incorporating catalyst synthesis with sorption materials. Hulteberg identified γ -zeolite and zeolite 4A as promising sorption materials in Work Package 3. γ -zeolite was then incorporated as a catalyst support for synthesis using supercritical flow method (Section 9, 10). Zeolite 4A was incorporated as a catalyst support for synthesis using both the ion-exchange and wetness impregnation methods (Section 12). Task 2.5 focused on upscaling the catalyst production for the plasma reactor. The established wetness impregnation method yielded 2-gram batches (Section 12). The wetness impregnation method was upscaled 10-, 50- and 100-gram batches (Section 13). This was achieved using various nickel catalyst alloys (Ni, NiCo, NiFe), and various promoters (Ca, Ba, La) supported on zeolite 4A.

All the tasks (T2.1-2.5) were addressed in work package 2 and the relevant milestones were reached. The first catalyst candidates (cobalt and nickel) were prepared for the enhanced plasma reactor (MS3). The decision on catalyst materials (promoted nickel alloys on 4A) was made (MS4). The production of these catalyst materials was upscaled to 100-gram batches (MS7). While there is room for more optimization, our investigations adequately addressed the objectives. This report therefore concludes Work Package 2.

15. References

1. Seong, G. *et al.* Supercritical hydrothermal synthesis of metallic cobalt nanoparticles and its thermodynamic analysis. in *Journal of Supercritical Fluids* vol. 60 113–120 (2011).
2. Kim, M. *et al.* Hydrothermal synthesis of metal nanoparticles using glycerol as a reducing agent. *Journal of Supercritical Fluids* 90, 53–59 (2014).
3. Mehta, P. *et al.* Overcoming ammonia synthesis scaling relations with plasma-enabled catalysis. *Nat Catal* 1, 269–275 (2018).
4. Sarraf, H. & Herbig, R. *Electrokinetic Sonic Amplitude Measurement of Concentrated Alumina Suspensions: Effect of Electrosteric Stabilization*. *Journal of the Ceramic Society of Japan* vol. 116 (2008).
5. Julian, I. *et al.* Supercritical solvothermal synthesis under reducing conditions to increase stability and durability of Mo/ZSM-5 catalysts in methane dehydroaromatization. *Appl Catal B* 263, (2020).
6. Otto, T., Zones, S. I., Hong, Y. & Iglesia, E. Synthesis of highly dispersed cobalt oxide clusters encapsulated within LTA zeolites. *J Catal* 356, 173–185 (2017).
7. Liu, Y. *et al.* A General Strategy for Fabricating Isolated Single Metal Atomic Site Catalysts in γ Zeolite. *J Am Chem Soc* 141, 9305–9311 (2019).

16. Appendix



This project has received funding from the European Union's Horizon Europe research and innovation programme under grant agreement No 101083905.



Part of this project has also received funding from UK Research and Innovation.